Hindawi
Advances in Civil Engineering
Volume 2018, Article ID 7987589, 11 pages
https://doi.org/10.1155/2018/7987589

Research Article

Use of Silica Fume and GGBS to Improve Frost Resistance of ECC with High-Volume Fly Ash

Yushi Liu,[1,2,3] Xiaoming Zhou,[1] Chengbo Lv,[1] Yingzi Yang,[1,2,3] and Tianan Liu[1]

[1]*School of Civil Engineering, Harbin Institute of Technology, Harbin 150090, China*
[2]*Key Lab of Structures Dynamic Behavior and Control of the Ministry of Education, Harbin Institute of Technology, Harbin 150090, China*
[3]*Key Lab of Smart Prevention and Mitigation of Civil Engineering Disasters of the Ministry of Industry and Information Technology, Harbin Institute of Technology, Harbin 150090, China*

Correspondence should be addressed to Yingzi Yang; yzyang@hit.edu.cn

Received 29 December 2017; Accepted 19 February 2018; Published 19 April 2018

Academic Editor: Peng Zhang

Fly ash (FA) has been an important ingredient for engineered cementitious composite (ECC) with excellent tensile strain capacity and multiple cracking. Unfortunately, the frost resistance of ECC with high-volume FA has always been a problem. This paper discusses the influence of silica fume (SF) and ground-granulated blast-furnace slag (GGBS) on the frost resistance of ECC with high volume of FA. Four ECC mixtures, ECC (50% FA), ECC (70% FA), ECC (30% FA + 40% SL), and ECC (65% FA + 5% SF), are evaluated by freezing-thawing cycles up to 200 cycles in tap water and sodium chloride solution. The result shows the relative dynamic elastic modulus and mass loss of ECC in sodium chloride solution by freeze-thaw cycles are larger than those in tap water by freeze-thaw cycles. Moreover, the relative dynamic elastic modulus and mass loss of ECC by freeze-thaw cycles increase with FA content increasing. However, the ECC (30% FA + 40% SL) shows a lower relative dynamic elastic modulus and mass loss, but its deflection upon four-point bending test is relatively smaller before and after freeze-thaw cycles. By contrast, the ECC (65% FA + 5% SF) exhibits a significant deflection increase with higher first cracking load, and the toughness increases sharply after freeze-thaw cycles, meaning ECC has good toughness property.

1. Introduction

In recent years, the development of high-performance cementitious (HPC) materials, including high-strength concretes with low water-cementitious materials ratio, and high-performance fiber-reinforced cementitious (HPFRC) composites has remarkable advancement. Green concrete is more environmentally friendly because it contains increasing contents of mineral admixtures and by-products. According to global sustainable development, green high-performance cementitious (GHPC) material is developed in the past years [1–3]. Using different mineral admixtures to partially replace cement is important [4–6] because it potentially reduces the pollution of industrial by-products and greenhouse gases [7].

The engineered cementitious composite (ECC) possesses high ductility and toughness under the shear and tension loading. The maximum tensile strain exceeds 3% when adding 2 vol.% fiber by micromechanical design [8–10]. Because coarse aggregates affect the distribution of fibers and weaken the interface transition zone within ordinary concrete, the brittleness of concrete is improved greatly by applying ECC without coarse aggregates [11]. Moreover, ECC has great ability in controlling crack width, and it has a number of applications, such as weight-bearing structures of concrete and steel-concrete composite airport runways and bridge decks, but the high strength and ductility of ECC are still stressed [12–14]. It is known that each ton of cement produced generates an equal amount of carbon dioxide, responsible for 5% of global greenhouse gas emission created by human activities [15]. Therefore, in view of global sustainable development, it is imperative to develop green ECC in which cement is replaced by supplementary cementitious

material (SCM) partially. Though the strength of ECC decreases with the addition of FA, the ductility and toughness are greatly improved. Moreover, hydration heat and cost are reduced because of FA replacing cement partially [5, 16].

In cold regions, concrete is subject to many freezing-thawing cycles every year. Hence, the freeze-thaw cycle is the main factor that damages the concrete structure in cold regions [17]. More seriously, in order to ensure safe driving, the sprinkle of deicing salt has further reduced the service life of the concrete. [18]. Yun and Rokugo [19] proved the abovementioned damage effects of freeze-thaw cycles as well as reinforcing fiber combination on flexural properties and cracking procedure of DFRCC prismatic specimens. Liu et al. [20] focused on the durability study on engineered cementitious composite (ECC) under sulfate and chloride environment. The freeze-thaw durability of high-strength concrete under deicer salt exposure was studied by Liu and Hansen [21]. The flexural impact performance, freeze-thaw, and deicing salt resistance of steel fiber-reinforced concrete were investigated by Zhang et al. [22]. Obviously, it is necessary to study the frost resistance of ECC with high-volume fly ash exposed to tap water and sodium chloride solution under freezing-thawing cycles.

However, the frost resistance on ECC blended with high-volume fly ash is not ideal. Özbay et al. [23] reported that an increase up to 70 wt.% in the FA replacement content was observed to exacerbate the deterioration of ECC mixtures caused by freezing-thawing cycles. The test results by Mustafa et al. [24] also showed the reduction of residual, physical, and mechanical properties with increasing number of freeze-thaw cycles is relatively more for ECC mixture with 70 wt.% FA than for ECC mixture with 55 wt.% FA, by weight of total cementitious material. And remarkably, only single supplementary cementitious material (SCM) was tried in their work.

GGBS is a replacement of cementitious material because of its availability in producing concrete and multi-performance concrete. GGBS provides advantages to concrete, lower permeability, higher sulfate and acid resistance, long-term strength, and lower heat of hydration [25]. Silica fume is an ultrafine amorphous powder of silicon dioxide with pozzolanic effect which fills the space among the cement particles to form a dense concrete matrix and interfacial transition zone (ITZ); this will increase the compressive strength and decrease the permeability of concrete [26–28]. Therefore, in view of the advantages of GGBS and silica fume, it is expected that the frost resistance and mechanical properties of ECC with high volume of fly ash will be improved by a certain amount of GGBS or silica fume replacing fly ash. And to the best of our knowledge, the attempts on the frost resistance improvement of ECC with high volume of fly ash by the binary supplementary cementitious materials (SCMs) have been lacking. Although Zhang and Li [29] investigated the durability of the concrete composite, with polypropylene fiber, containing fly ash and silica fume, the replacement level of fly ash was merely 15%, by weight of total cementitious material.

In this work, in order to present the ECC with good frost resistance, the ECC with 50 wt.% FA, 70 wt.% FA, 30 wt.% FA + 40 wt.% GGBS, and 65 wt.% FA + 5 wt.% SF is designed. Experimental tests consisted of measuring the change in mass and relative dynamic elastic modulus and residual compressive as well as flexural properties of ECC specimens exposed to the tap water and sodium chloride solution under freezing-thawing cycles up to 200. In addition, the four-point bending test after various freezing-thawing cycles was examined as well.

2. Experimental Section

2.1. Materials and Mix Proportions. In this study, the ingredients used in the production of ECC mixtures include P·O 42.5 Portland cement (PC), fly ash (FA), ground-granulated blast-furnace slag (GGBS), silica fume (SF), and microsilica sand with an average grain size and modulus of 150 μm and 2.01, respectively, water, polyvinyl alcohol (PVA) fibers, and superplasticizer. Physical properties and chemical compositions of PC and FA are listed in Table 1. The PVA fibers are 8 mm in length with the diameter of 39 μm. Tensile strength and density of PVA fiber are 1600 MPa and 1300 kg/m^3, respectively. The mixture proportions are presented in Table 2. ECC mixtures containing 50 wt.% and 70 wt.% FA, and 30 wt.% FA + 40 wt.% GGBS and 65 wt.% FA + 5 wt.% SF (by weight of total cementitious material) as a replacement of cement are prepared. The water to binder ratio (W/B) was fixed at 0.25.

2.2. Mixtures and Specimen Preparation. Before adding water, all the solid ingredients, including PC, FA, GGBS, SF, and sand, are firstly mixed for 2 min. Then, water and superplasticizer are added into dry mixture and mixed for another 2 min. PVA fibers are slowly added into mortar and mixed until all fibers are uniformly distributed. ECC mixtures are cast into molds and demolded after 24 h. ECC specimens are cured for 28 days in a standard curing room where temperature and relative humidity (RH) are 20 ± 0.5°C and 95 ± 5%, respectively, and then, the freezing and thawing tests are conducted on ECC specimens by water-saturated treatment. For each ECC mix, plate-shaped specimens of 12 mm × 40 mm × 320 mm are used to conduct the four-point bending test. Prism specimens of 160 mm × 40 mm × 40 mm are prepared for compressive strength and flexural strength, respectively.

2.3. Frost Resistance Test Procedures. A freezing and thawing testing apparatus satisfying the ASTM C666 Procedure A requirements was used for testing. The specimens of 100 mm × 100 mm × 400 mm were prepared for the tests in the loss of mass and relative dynamic elastic modulus, and the specimens of 12 mm × 40 mm × 320 mm were prepared for the tests in the toughness of ECC. All of the specimens were subjected to 200 freezing and thawing cycles, which included 5~6 freezing and thawing cycles in a 24 h period. The specimen was removed after 28 days of maintenance in the standard curing room; then it was submerged in tap water for 3 days; and finally it was tested under the freeze-thaw treatment of tap water or 3% (by mass) sodium

Table 1: Physical properties and chemical compositions of raw materials.

Chemical composition (%)	PC	FA	SL	SF	Physical properties	PC	FA	SL	SF
CaO	62.28	2.93	26.6	0.33	Loss on ignition (%)	1.61	3.03	0.40	—
SiO_2	21.08	65.7	34.18	90.54	Average particle size (μm)	—	3.4	1.7	—
Al_2O_3	5.47	20.63	13.8	0.77	Density (g/cm^3)	3.18	2.43	2.85	—
MgO	1.73	2.25	9.15	1.68	Specific surface area (m^2/kg)	—	655	476	23000
Fe_2O_3	3.96	4.65	15.32	1.77					
SO_3	2.63	0.28	0.50	0.40					

Table 2: Mix proportion and properties of ECC (kg/m^3).

Mix number	Water	Cement	FA	GGBS	SF	Sand	Fiber	Superplasticizer
Control mortar	318	636	636 (50%)	—	—	462	—	6
ECC (50% FA)	318	636	636 (50%)	—	—	462	26	18
ECC (70% FA)	318	382	890 (70%)	—	—	462	26	16
ECC (30% FA + 40% SL)	318	382	381 (30%)	509 (40%)	—	462	26	15
ECC (65% FA + 5% SF)	318	382	826 (65%)	—	64 (5%)	462	26	15

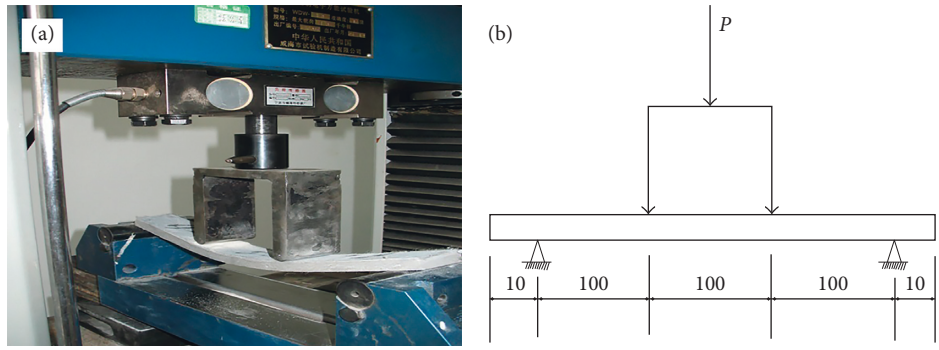

Figure 1: (a) Four-point bending test setup for ECC. (b) Loading device schematic.

chloride solution. After a certain number of freeze-thaw cycles, the loss of mass and relative dynamic elastic modulus were checked, and both the sodium chloride solution and tap water were renewed; the compressive strength, flexural strength, and toughness of ECC were obtained as well.

The flexural strength and compressive strength for each mix were measured according to GB/T 17671-1999. The size of the specimen is 40 mm × 40 mm × 160 mm for the flexural strength test. Averages of the three specimens for each mix were reported as the results of flexural strength after the three-point flexural test was conducted at a loading rate of 50 N/s. Six broken samples were used to measure compressive strength with a loading rate of 1.5 kN/s after the flexural test. The average of six samples for each mixture was reported as the tested compressive strength.

As shown in Figure 1, the four-point bending test is performed under displacement control at a loading rate of 1.0 mm/min. The first cracking load, the load-deflection behavior, and toughness can be obtained from this test.

3. Results and Discussion

3.1. Relative Dynamic Elastic Modulus and Mass Loss. The relative dynamic elastic modulus and mass loss after freeze-thaw cycles are carried out to evaluate the frost resistant performance of cementitious composite materials. Figures 2(a) and 2(b) show the change of the dynamic modulus and mass of the sample, respectively. In Figure 2, the dynamic elastic modulus of the control mortar decreases by 23.4% after 75 freeze-thaw (F-T) cycles in tap water, and decreasing by 45.73% after 100 water freeze-thaw (F-T) cycles, indicating the interior of the sample has been greatly damaged by freeze-thaw cycles. By comparison, the dynamic elastic moduli of all the ECC are basically unchanged, and their masses have slightly increased. This can be explained as follows: the measuring results of air contents show that the air contents of fresh control mortar, ECC (50% FA), ECC (70% FA), ECC (30% FA + 40% SL), and ECC (65% FA + 5% SF), are 3.0%, 7.3%, 7.7%, 8.0%, and 7.5%, respectively. That is, the incorporation of fiber will entrap more air bubbles in the mortar matrix, the number of pores of ECC is higher than that of control mortar, and the pores can relieve the stress due to the freeze-thaw cycles, improving the frost resistance of ECC. Moreover, it is more favorable for the continuous hydration of ECC in the water, leading to the slow growth in the mass of ECC.

After 200 water F-T cycles, the dynamic elastic modulus of ECC (50% FA) decreases by 1.79%, and its mass increases

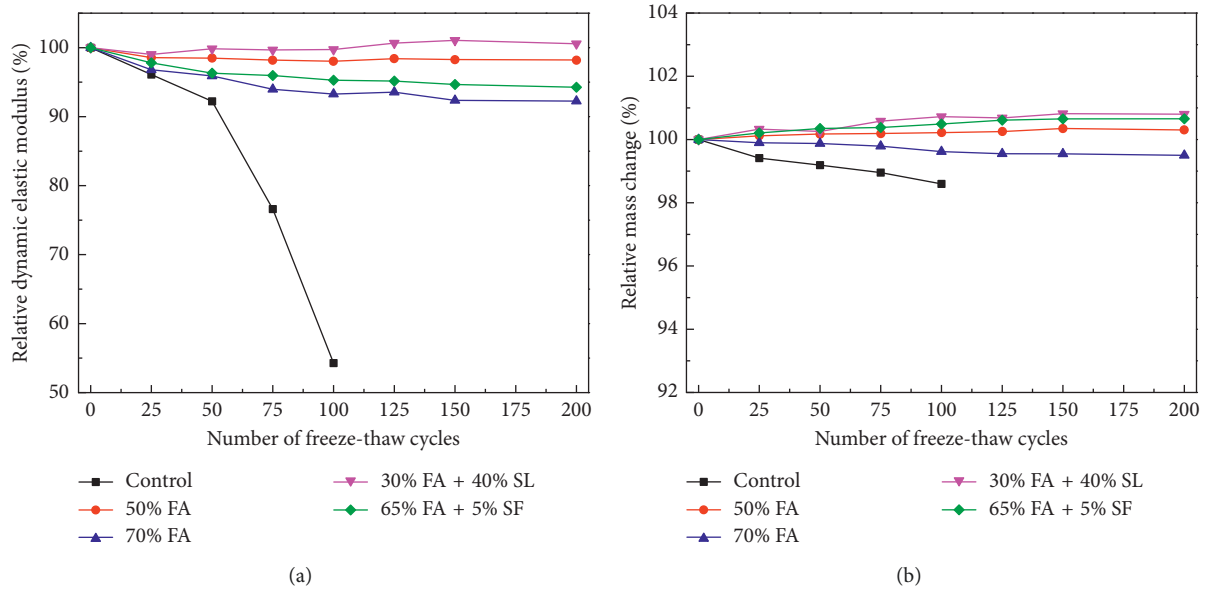

Figure 2: (a) Relative dynamic elastic modulus. (b) Relative mass change versus under freeze-thaw cycles in tap water.

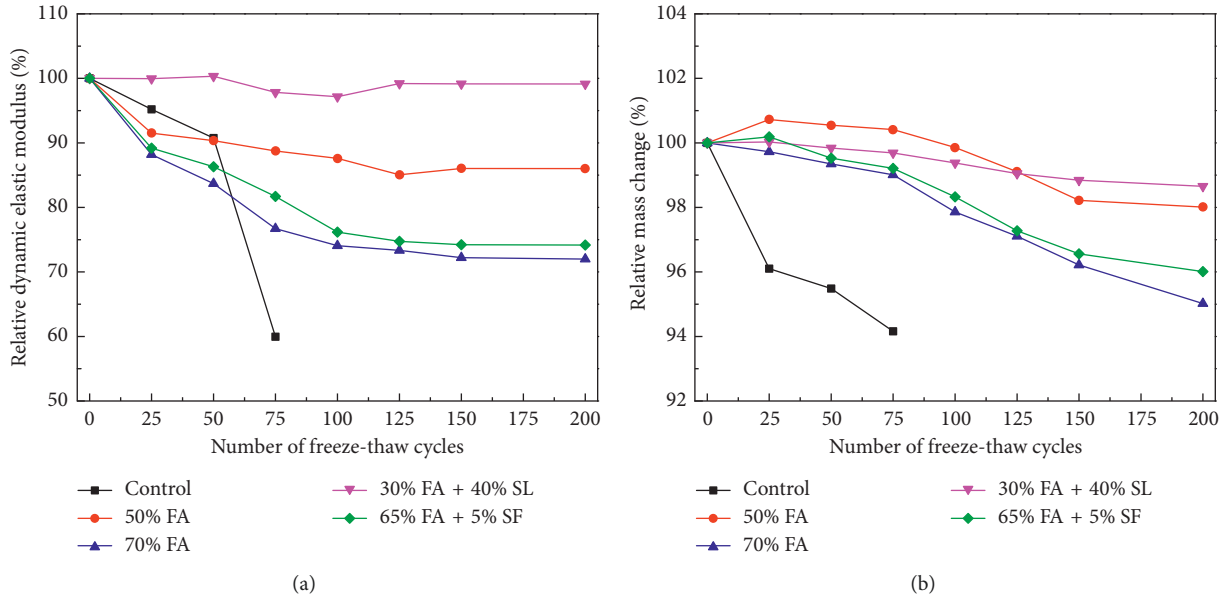

Figure 3: (a) Relative dynamic elastic modulus. (b) Relative mass change under freeze-thaw cycles in sodium chloride solution.

by 0.30%; the dynamic elastic modulus of ECC (70% FA) decreases by 7.74%, and its mass decreases by 0.50%. Apparently, with the increasing FA content, the frost resistance of ECC gets worse, which is related to the decreased strength because of the increased additive amount of FA. However, the dynamic elastic modulus of ECC (30% FA + 40% SL) increases by 0.57%, and its mass increases by 0.80%; the dynamic elastic modulus of ECC (65% FA + 5% SF) decreases by 5.74%, and its mass increases by 0.66%. It is found that ECC (30% FA + 40% SL) and ECC (65% FA + 5% SF) show better frost resistance compared with ECC (70% FA). This is attributed to GGBS and SF contributing to the strength improvement of ECC (70% FA). The detailed discussions for the strengths of ECC can be found in Sections 3.2 and 3.3.

Figures 3(a) and 3(b) show the changes of the dynamic elastic modulus and mass of the specimen after freezing and thawing in sodium chloride solution, respectively. The mass of control mortar decreases by 5.84% after 75 freeze-thaw (F-T) cycles, and the dynamic elastic modulus decreases by 40%. Thus, the control mortar is not available. For all the ECC with F-T cycles in sodium chloride solution, their dynamic elastic modulus and mass developments are similar to those with F-T cycles in tap water. However, the damaging effects with sodium chloride solution on the dynamic elastic modulus and mass are more serious than that with tap water.

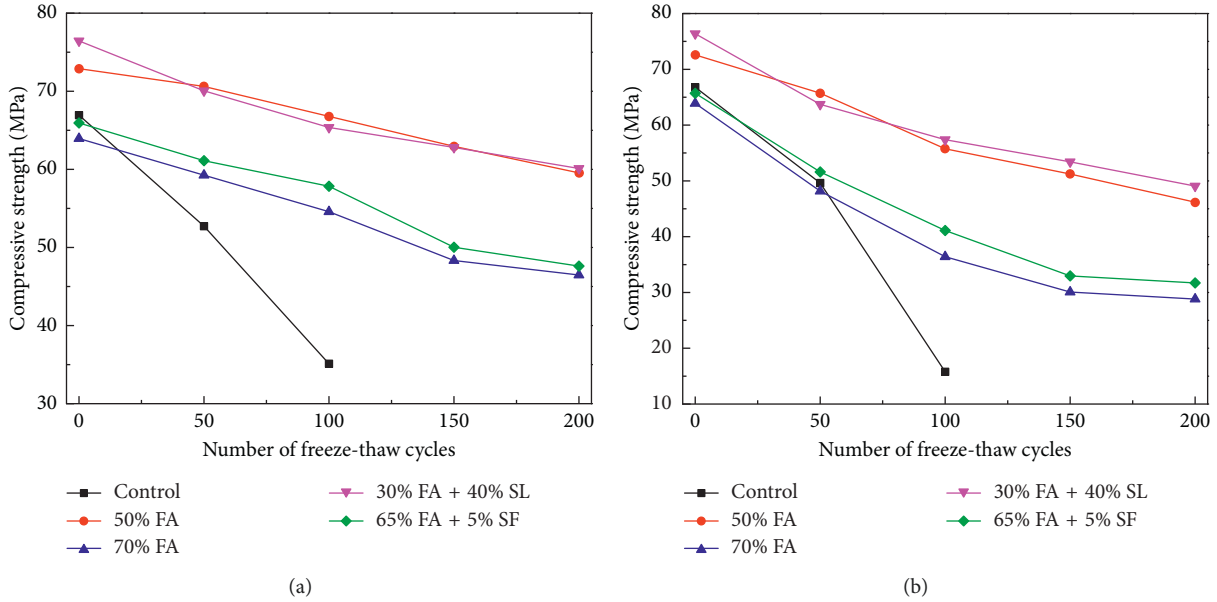

Figure 4: Compressive strength under freeze-thaw cycles: (a) in tap water and (b) in sodium chloride solution.

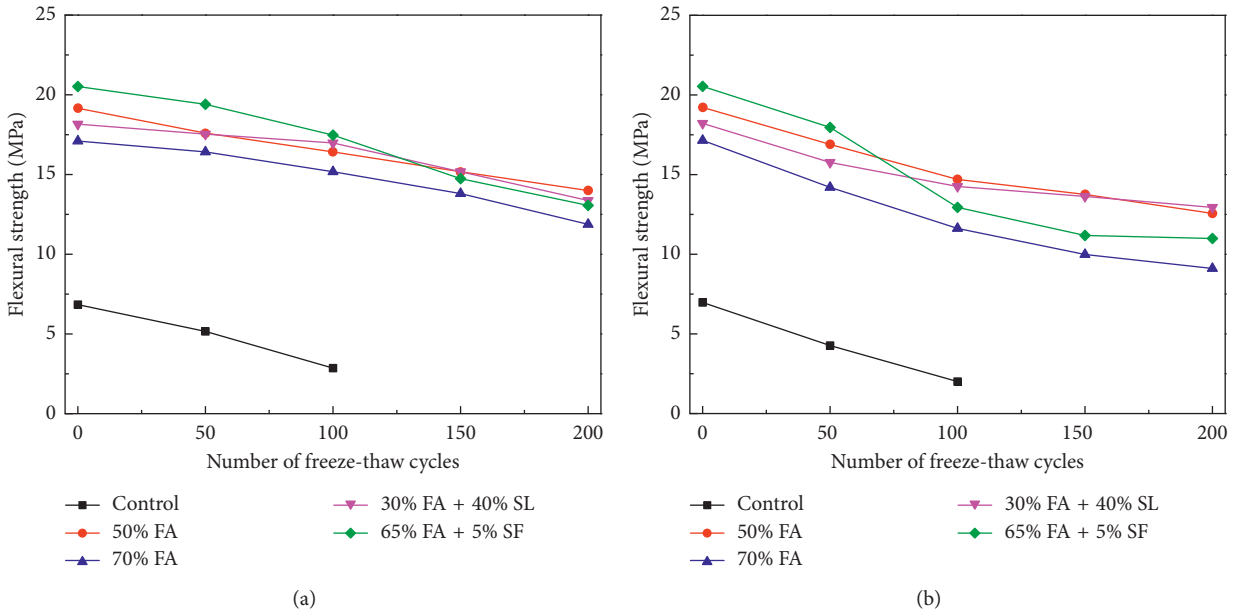

Figure 5: Flexural strength under freeze-thaw cycles: (a) in tap water and (b) in sodium chloride (NaCl) solution.

This is due to the fact that when in contact with sodium chloride solution, the chemical reactions between chloride ions and cement hydration products create expansion component, leading to crack formation of ECC mixtures. Cracks in ECC mixtures allow the chloride ions to penetrate into the interior of the structure, further accelerating the deterioration [30, 31].

3.2. Compressive Behavior of ECC. Figures 4(a) and 4(b) show the compressive strength subjected to freeze-thaw (F-T) cycles in tap water and salt solution, respectively. The influence of freeze-thaw (F-T) cycles on ECC and the control mortar is obvious from Figure 4. The decrease of compressive strength is obvious, especially the specimen subjected to F-T cycles in salt solution, because the specimen is damaged severely in salt solution. The compressive strength of control mortar decreases by 47.3% in tap water and 76.2% in salt solution after 100 freeze-thaw (F-T) cycles; thus the control mortar is not available because of the serious damage after 100 freeze-thaw cycles. Additionally, after 200 F-T cycles in tap water, the compressive strength of ECC (50% FA) decreases by 18.0%; the compressive strength of ECC (70% FA) decreases by 27.2%; the compressive strength of ECC (30% FA

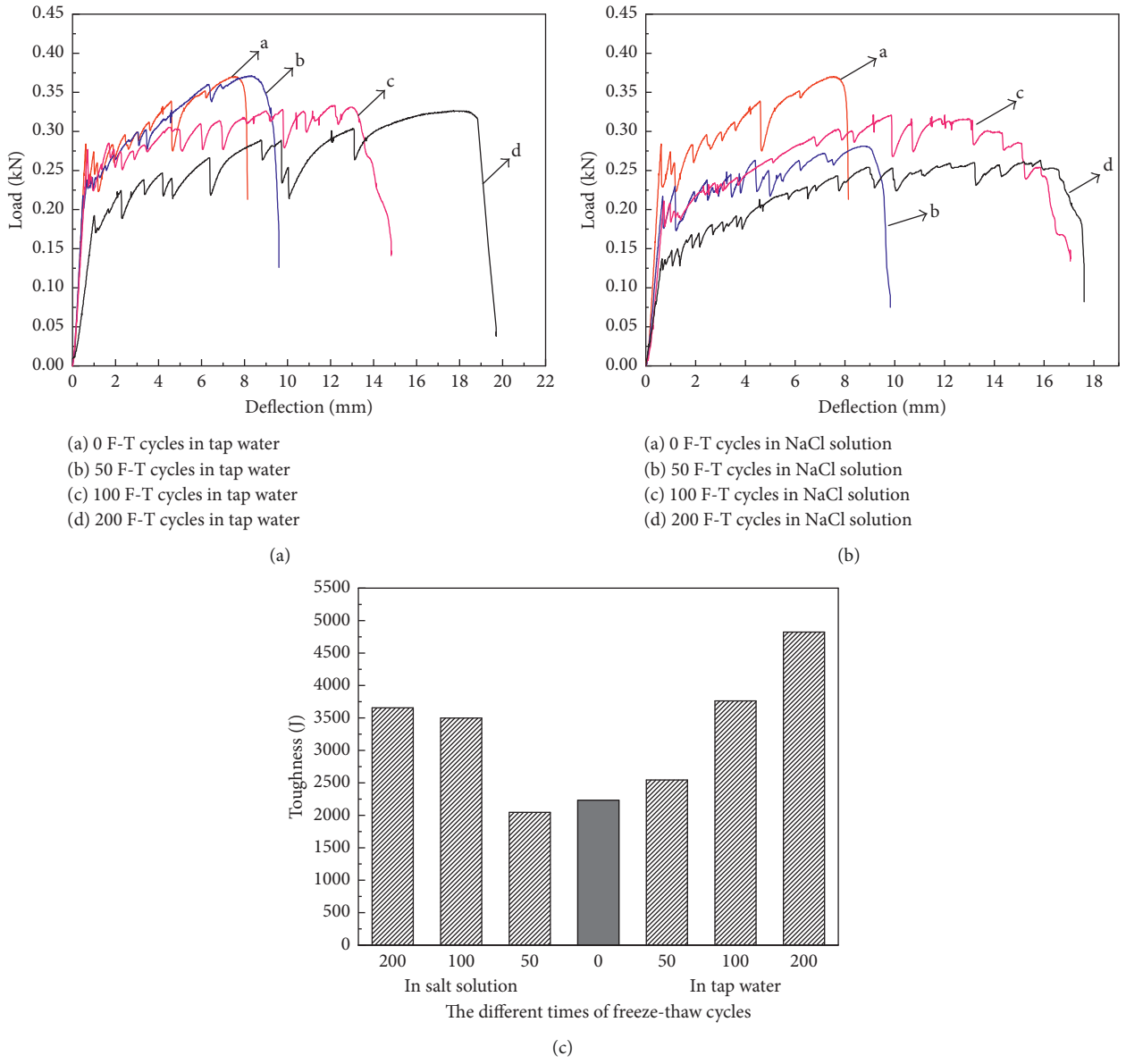

Figure 6: The load-deflection of ECC (50% FA) subjected to different freeze-thaw cycles: (a) in tap water, (b) in sodium chloride (NaCl) solution, and (c) the corresponding toughness with different times of freeze-thaw cycles.

+ 40% SL) decreases by 21.4%; and the compressive strength of ECC (65% FA + 5% SF) decreases by 27.9%. For all the ECC with F-T cycles in salt solution, their compressive strength developments are similar to those with F-T cycles in tap water. Obviously, whether in tap water or salt solution, ECC samples show less loss of compression strength than that of control mortar after freeze-thaw cycles.

3.3. Flexural Behavior of ECC. Figures 5(a) and 5(b) show the flexural strengths of samples by freeze-thaw cycles in tap water and salt solution. respectively. The influence of freeze-thaw (F-T) cycles on the flexural strength of ECC and the control mortar can be clearly seen from Figure 5. The flexural strength of control mortar decreases by 57.1% in tap water and 70.0% in salt solution after 100 freeze-thaw (F-T) cycles; thus the control mortar is not available because of the serious damage after 100 freeze-thaw cycles. Being similar to the compressive strength, it also shows the superior flexural strength of ECC. The reasons are presented as follows. (1) The frost resistance of the ECC is far better than control because of the PVA fiber blending, and the freeze-thaw cycles have not severe influence on the strength of ECC. (2) The addition of PVA fiber greatly enhances flexural strength of ECC because of the bridging effect of PVA fiber.

Before freeze-thaw (F-T) cycles, it can be seen from Figure 5(a) that as the FA content further increases from 50 wt.% to 70 wt.%, the flexural strength of ECC decreases from 19.2 MPa to 17.1 MPa. However, the flexural strengths of ECC (30% FA + 40% SL) and ECC (65% FA + 5% SF) are

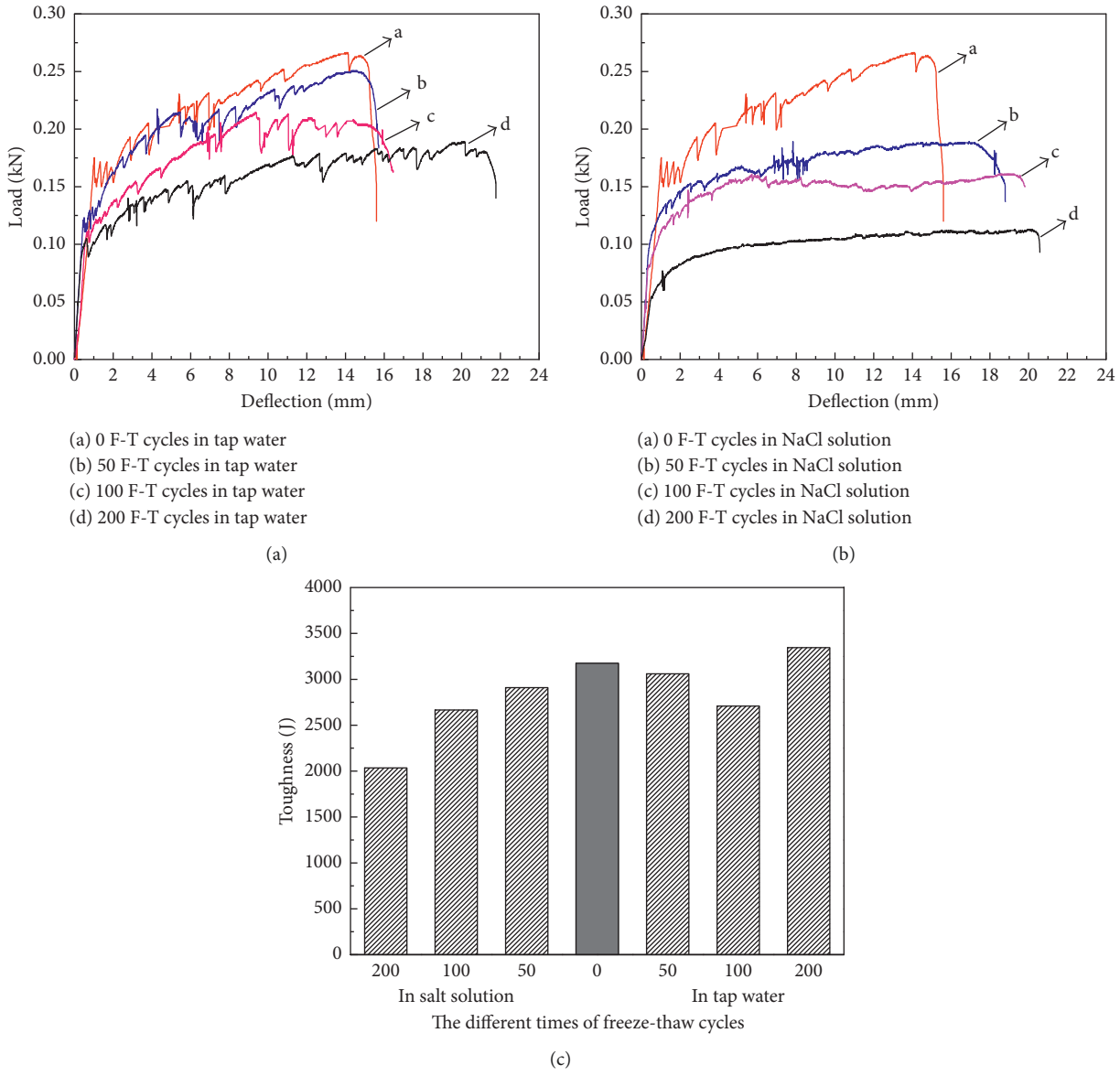

Figure 7: The load-deflection of ECC (70% FA) subjected to different times of freeze-thaw cycles: (a) in tap water, (b) in sodium chloride (NaCl) solution, and (c) the corresponding toughness with different times of freeze-thaw cycles.

over than that of ECC (70% FA) because of the addition of GGBS and SF. Although the flexural strength has decreased with increasing the number of freeze-thaw cycles, especially the specimens subjected to F-T cycles in salt solution, ECC (30% FA + 40% SL) and ECC (65% FA + 5% SF) still show a higher flexural strength compared with ECC (70% FA). Moreover, the flexural strength of ECC (30% FA + 40% SL) is higher than that of ECC (65% FA + 5% SF) after 200 freeze-thaw cycles in tap water and salt solution.

Compared with other's results [32], one reason of the relative lower compressive strength and flexural strength of ECC after F-T cycles may be attributed to the size effects of the ECC specimen. Smaller specimen size results in more serious damage effects [33]. However, as a comparison of testing results among different ECC mix, the conclusions are still trustworthy.

3.4. Toughness Behavior of ECC. Toughness is the ability of a material to absorb energy and plastically deform without fracturing. For ECC mixtures, the toughness can be defined as a resistance to fracture when stressed. Toughness can be determined by integrating the stress-strain curve. It is the energy of mechanical deformation per unit volume prior to fracture. And toughness requires a balance of strength and ductility [34]. Figures 6(a) and 6(b) show the load-deflection curve of ECC (50% FA) by freeze-thaw cycles in tap water and sodium chloride solution, respectively. The corresponding toughnesses are displayed in Figure 6(c).

From Figures 6(a) and 6(b), the first cracking load declines and the maximum deflection increases with increasing number of F-T cycles in tap water and sodium chloride solution. Figure 6(a) shows the load-deflection curve of ECC (50% FA) with different F-T cycles in tap water. Before F-T

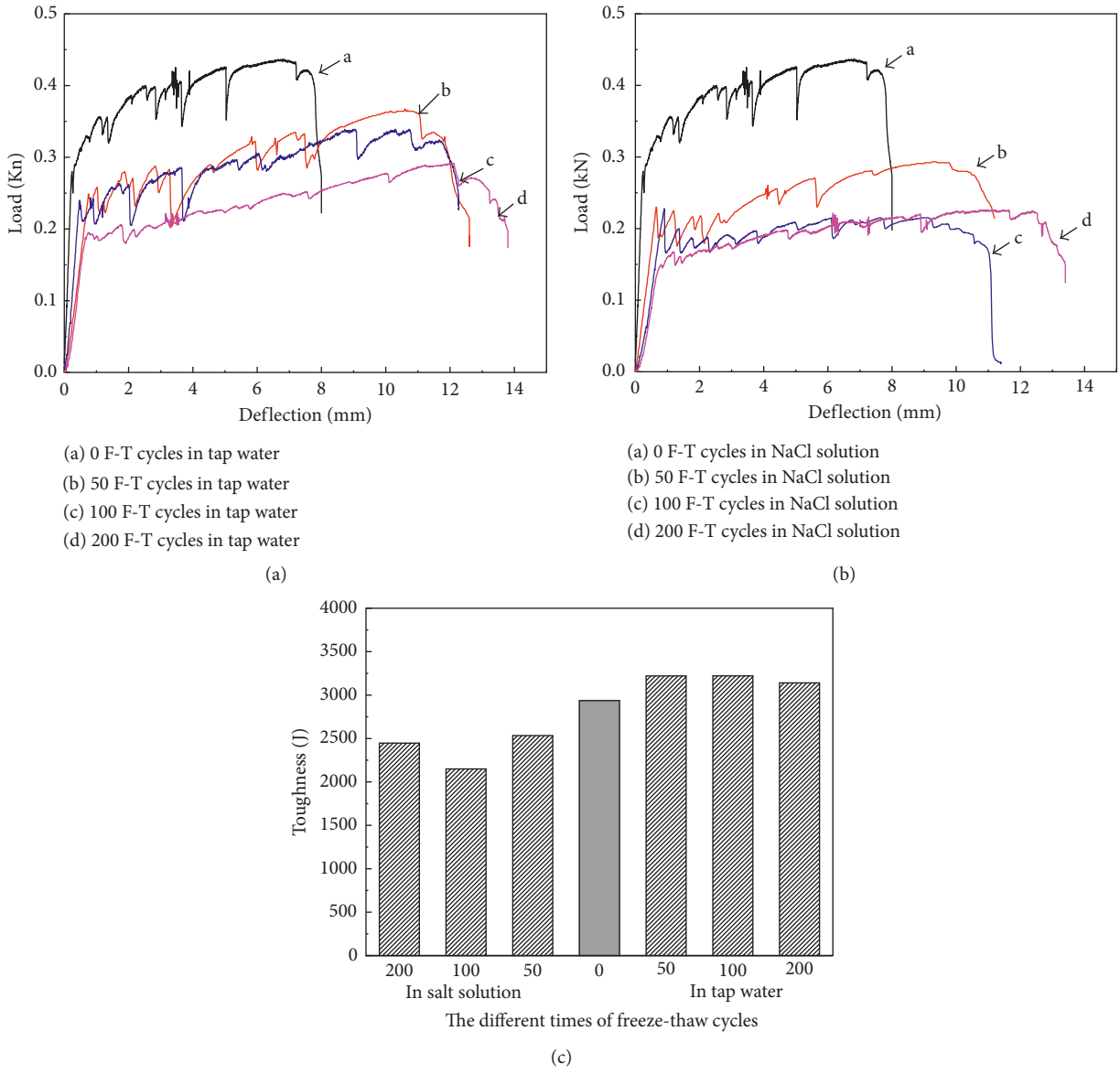

Figure 8: The load-deflection of ECC (30% FA + 40% SL) subjected to different times of freeze-thaw cycle: (a) in tap water, (b) in sodium chloride (NaCl) solution, and (c) the corresponding toughness with different times of freeze-thaw cycles.

cycles, the first cracking load and deflection are 284 N and 7.59 mm, respectively. And the first cracking load decreases to 192 N and the maximum deflection increases to 18.50 mm after 200 F-T cycles in tap water. Obviously, F-T cycles have a damaging effect on the strength of ECC (50% FA) but contribute to its ductility. In addition, the first cracking load decreases to 137 N and the maximum deflection increases to 16.51 mm after 200 F-T cycles in sodium chloride solution. It is found that the first cracking load in sodium chloride is much lower than that in tap water, indicating the freeze-thaw action is more important to failure of ECC (50% FA) compared with the action of deicing salt. However, there is only little difference between the ductility of ECC (50% FA) in sodium chloride and tap water. From Figure 6(c), the toughness decreases slightly and then increases with the number of F-T cycles in sodium chloride solution, and it increases continuously with the number of F-T cycles in tap water. After 200 F-T cycles, the toughness in tap water is 4823.5 J which is higher than 3656.6 J of toughness in sodium chloride solution, indicating that the F-T cycles in tap water is beneficial to the development of toughness compared with that in sodium chloride solution.

Figures 7(a) and 7(b) show the load-deflection curve of ECC (70% FA) by freeze-thaw cycles in tap water and sodium chloride solution, respectively. The corresponding toughnesses are displayed in Figure 7(c). From Figures 7(a) and 7(b), the first cracking load of ECC (70% FA) reduces significantly compared to that of ECC (50% FA) after 200 F-T cycles. For example, the first cracking load decreases to 71 N after 200 F-T cycles in sodium chloride solution. This first cracking load value is too lower to be used in the practical engineering. However, the maximum deflection of

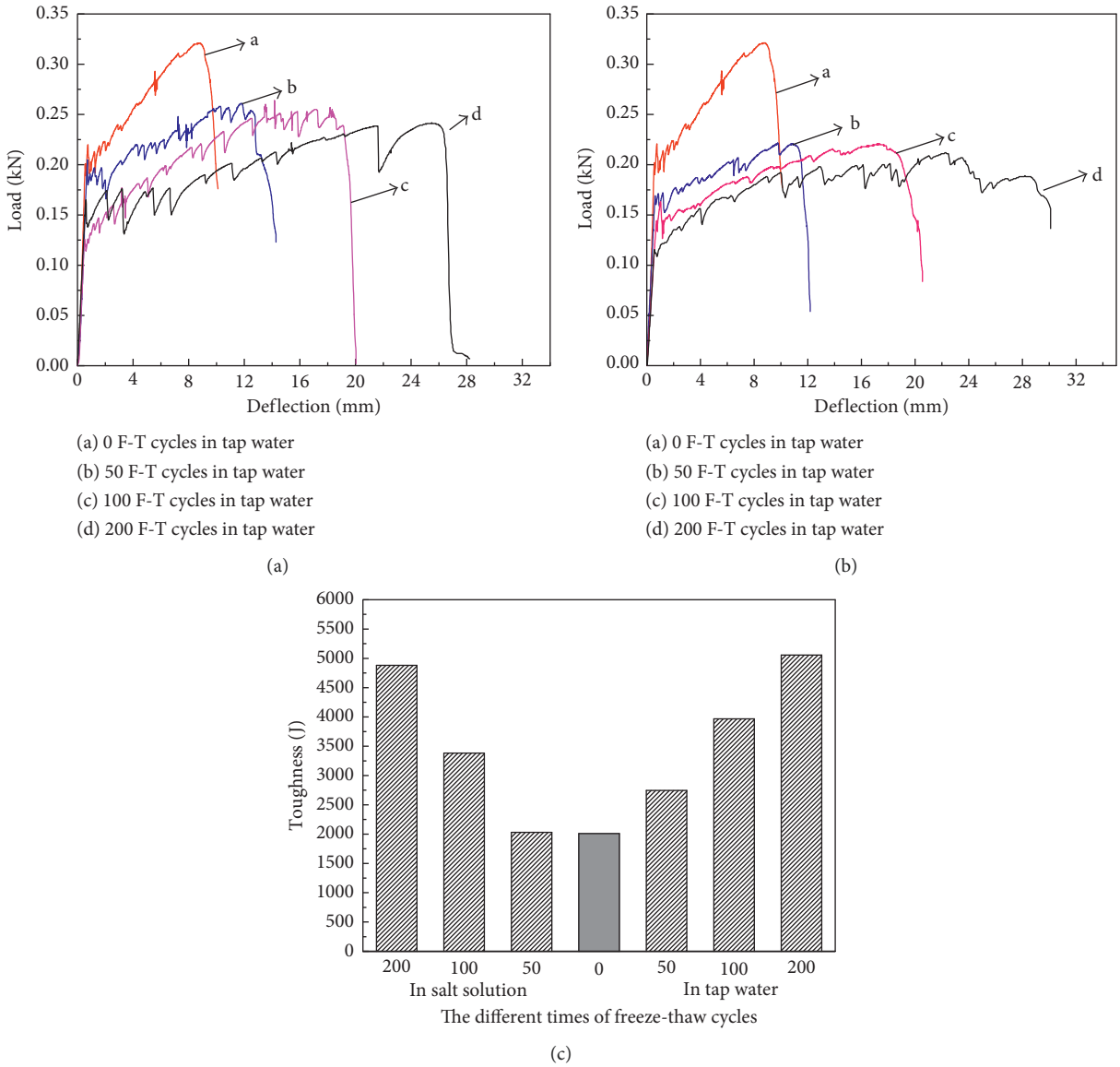

Figure 9: The load-deflection of ECC (65% FA + 5% SF) subjected to different times of freeze-thaw cycle: (a) in tap water, (b) in sodium chloride (NaCl) solution, and (c) the corresponding toughness with different times of freeze-thaw cycles.

ECC (70% FA) shows a further increase of 3~4 mm compared with that of ECC (50% FA) in tap water and sodium chloride solution, showing an excellent ductility which has distinct advantages in application. FA has significant contribution to improve ductility of ECC, which is attributed to the reduction in the PVA fiber/matrix interface chemical bond and matrix toughness and the increase in the interface frictional bond [35]. From Figure 7(c), the toughness of ECC (70% FA) decreases continuously with the number of F-T cycles in sodium chloride solution, and the minimum toughness is as low as 2034.5 J. Moreover, the increase of its toughness has quite weak growth with the number of F-T cycles in sodium chloride solution, indicating the poor toughness property.

In order to improve the strength and durability of ECC with high-volume fly ash, GGBS and SF were added into ECC (70% FA), in which GGBS and SF were used as the ingredient of ECC-FA mixture, and the replacement levels are 30 wt.% and 5 wt.%, by weight of total cementitious material, respectively. For the toughness behavior of ECC (30% FA + 40% SL) and ECC (65% FA + 5% SF), the details are discussed as follows.

Figures 8(a) and 8(b) show the load-deflection curve of ECC (30% FA + 40% SL) by freeze-thaw cycles in tap water and sodium chloride solution, respectively. The corresponding toughnesses are displayed in Figure 8(c). From Figures 8(a) and 8(b), the first cracking load of ECC (30% FA + 40% SL) is a little higher than that of ECC (50% FA) after 200 F-T cycles. For example, the first cracking load increases from 137 N and 71 N of ECC (50% FA) and ECC (70% FA) to 150 N of ECC (30% FA + 40% SL) after 200 F-T cycles in sodium chloride solution. However, the maximum

deflection of ECC (30% FA + 40% SL) is lower than that of ECC (50% FA). After 200 F-T cycles in sodium chloride solution, the maximum deflection of ECC (30% FA + 40% SL) decreases by about 24% compared to that of ECC (50% FA) and decreases by 40% compared to that of ECC (70% FA). Obviously, the increase in the strength of ECC (30% FA + 40% SL) by addition of GGBS is based on the sacrifice of the ductility. Furthermore, the toughness of ECC (30% FA + 40% SL) decreases but does not show the distinct change with the number of F-T cycles in sodium chloride solution.

Figures 9(a) and 9(b) show the load-deflection curve of ECC (65% FA + 5% SF) by freeze-thaw cycles in tap water and sodium chloride solution, respectively. The corresponding toughnesses are displayed in Figure 9(c). From Figures 9(a) and 9(b), before F-T cycles, the first cracking load and deflection are 220 N and 8.86 mm, respectively. The first cracking load decreases to 161 N and the maximum deflection increases to 25.75 mm after 200 F-T cycles in tap water. Moreover, the first cracking load decreases to 115 N and the maximum deflection increases to 28.19 mm after 200 F-T cycles in sodium chloride solution. With the increase of the number of F-T cycles, the first cracking load is decreased, but the deflection value and toughness keep increasing. Additionally, the initial crack load is stable and fluctuates within a certain range. The maximum deflection of ECC (65% FA + 5% SF) after 200 F-T cycles is 3 times over that before F-T cycles, showing an outstanding ductility. Moreover, taking sodium chloride solution, for example, the first cracking load increases from 71 N of ECC (70% FA) to 115 N of ECC (65% FA + 5% SF) after 200 F-T cycles, and the growth rate increases to 38.3%. In addition, the toughness of ECC (65% FA + 5% SF) increases continuously with the number of F-T cycles in both tap water and sodium chloride solution. This is very beneficial to its application performance. Therefore, it is not difficult to draw the conclusion that ECC (65% FA + 5% SF) has a good frost resistance with better strength and durability, which is a promising ECC mixture if the toughness of material is the most important design parameter.

4. Conclusions

The following conclusions have been highlighted from the study:

(1) The maximum deflection increases markedly when the FA content increases from 50 wt.% to 70 wt.% in the ECC mixtures, but the compressive strength and the first cracking load have been a sharp decline. However, GGBS and SF distinctly improve the mechanical properties of ECC with fly ash. For instance, the compressive strength, flexural strength, and first cracking load of ECC (30% FA + 40% SL) are higher than those of ECC (50% FA). Remarkably, the abovementioned mechanical properties of ECC (65% FA + 5% SF) are similar to those of ECC (70% FA).

(2) The results for the losses of compressive strength, flexural strength, relative dynamic elastic modulus, and mass in the control mortar demonstrate that the control mortar cannot withstand the actions of 100 freeze-thaw cycles. By contrast, the four ECC mixes show a better frost resistance than control mortar. During the process of freeze-thaw, the damaging effects of sodium chloride solution on ECC and control mortar are more obvious than that of tap water.

(3) Based on the relative dynamic elastic modulus, mass loss, and change of toughness under the freeze-thaw cycles, ECC (30% FA + 40% SL) shows better frost resistance compared to ECC (50% FA) and ECC (70% FA), whereas the frost resistance of ECC (65% FA + 5% SF) is stronger than that of ECC (70% FA). After 200 F-T cycles, the maximum deflection of ECC (70% FA) is 3 times over that before F-T cycles, showing an excellent ductility.

Furthermore, how to improve the frost resistance of ECC in a service environment with a deicing salt should be an important research task in the near future.

Conflicts of Interest

The authors declare that there are no conflicts of interest regarding the publication of this paper.

Acknowledgments

This work was supported by the National Natural Science Foundation of China (no. 51578193).

References

[1] Z. Wu, "Green high performance concrete—the trend of concrete development," *Chinal Concrete and Cement Products*, vol. 1, pp. 3–6, 1998.

[2] N. Zhang, H. Li, Y. Zhao, and X. Liu, "Hydration characteristics and environmental friendly performance of a cementitious material composed of calcium silicate slag," *Journal of Hazardous Materials*, vol. 306, pp. 67–76, 2016.

[3] P. Zhang, Q. Li, and Z. Sun, "Influence of silica fume and polypropylene fiber on fracture properties of concrete composite containing fly ash," *Journal of Reinforced Plastics and Composites*, vol. 30, no. 24, pp. 1977–1988, 2011.

[4] M. Barboiu, E. Petit, D. L. A. Van, and G. Vaughan, "Experimental application of mineral admixtures in lightweight concrete with high strength and workability," *Construction and Building Materials*, vol. 22, no. 6, pp. 1108–1113, 2008.

[5] K. Tosun-Felekoğlu, E. Gödek, M. Keskinateş, and B. Felekoğlu, "Utilization and selection of proper fly ash in cost effective green HTPP-ECC design," *Journal of Cleaner Production*, vol. 149, pp. 557–568, 2017.

[6] P. Zhang, Q. Li, and H. Zhang, "Combined effect of polypropylene fiber and silica fume on mechanical properties of concrete composite containing fly ash," *Journal of Reinforced Plastics and Composites*, vol. 30, no. 16, pp. 1349–1358, 2011.

[7] K. Neupane, ""Fly ash and GGBFS based powder-activated geopolymer binders: a viable sustainable alternative of Portland cement in concrete industry," *Mechanics of Materials*, vol. 103, pp. 110–122, 2016.

[8] V. C. Li, "On Engineered Cementitious Composites (ECC): a review of the material and its applications," *Transportation*

Research Record Journal of the Transportation Research Board, vol. 2164, pp. 1–8, 2010.

[9] S. Wang, C. Wu, and V. C. Li, "Tensile strain-hardening behavior of polyvinyl alcohol engineered cementitious composite (PVA-ECC)," *ACI Materials Journal*, vol. 98, no. 6, pp. 483–492, 2001.

[10] V. C. Li and H. Wu, "Conditions for pseudo strain-hardening in fiber reinforced brittle matrix composites," *Applied Mechanics Reviews*, vol. 45, no. 8, p. 390, 2011.

[11] M. A. Chowdhury, M. M. Islam, and Z. I. Zahid, "finite element modeling of compressive and splitting tensile behavior of plain concrete and steel fiber reinforced concrete cylinder specimens," *Advances in Civil Engineering*, vol. 2016, Article ID 6579434, 11 pages, 2016.

[12] X. Shao, D. Yi, Z. Huang, H. Zhao, B. Chen, and M. Liu, "Basic performance of the composite deck system composed of orthotropic steel deck and ultrathin RPC layer," *Journal of Bridge Engineering*, vol. 18, no. 5, pp. 417–428, 2013.

[13] W. Zhenbo, Z. Jun, W. Jiahe, and S. Zhengjie, "Tensile performance of polyvinyl alcohol-steel hybrid fiber reinforced cementitious composite with impact of water to binder ratio," *Journal of Composite Materials*, vol. 49, no. 18, pp. 1–19, 2014.

[14] J. Zhang, Z. Wang, X. Ju, and Z. Shi, "Simulation of flexural performance of layered ECC-concrete composite beam with fracture mechanics model," *Engineering Fracture Mechanics*, vol. 131, pp. 419–438, 2014.

[15] H. G. Oss and A. C. Padovani, "Cement manufacture and the environment: part I: chemistry and technology," *Journal of Industrial Ecology*, vol. 6, no. 1, pp. 89–105, 2002.

[16] J. Yu, J. Lin, Z. Zhang, and V. C. Li, "Mechanical performance of ECC with high-volume fly ash after sub-elevated temperatures," *Construction and Building Materials*, vol. 99, pp. 82–89, 2015.

[17] K. Šeps, J. Fládr, and I. Broukalová, "Resistance of recycled aggregate concrete to freeze-thaw and deicing salts," *Procedia Engineering*, vol. 151, pp. 329–336, 2016.

[18] Z. Liu and W. Hansen, "Freezing characteristics of air-entrained concrete in the presence of deicing salt," *Cement and Concrete Research*, vol. 74, pp. 10–18, 2015.

[19] H. D. Yun and K. Rokugo, "Freeze-thaw influence on the flexural properties of ductile fiber-reinforced cementitious composites (DFRCCs) for durable infrastructures," *Cold Regions Science and Technology*, vol. 78, pp. 82–88, 2012.

[20] H. Liu, Q. Zhang, V. Li, H. Su, and C. Gu, "Durability study on engineered cementitious composites (ECC) under sulfate and chloride environment," *Construction and Building Materials*, vol. 133, pp. 171–181, 2017.

[21] Z. Liu and W. Hansen, "Freeze–thaw durability of high strength concrete under deicer salt exposure," *Construction and Building Materials*, vol. 102, pp. 478–485, 2016.

[22] W. Zhang, N. Zhang, and Y. Zhou, "Effect of flexural impact on freeze–thaw and deicing salt resistance of steel fiber reinforced concrete," *Materials and Structures*, vol. 49, no. 12, pp. 1–8, 2016.

[23] E. Özbay, M. Şahmaran, M. Lachemi, and H. E. Yücel, "Effect of microcracking on frost durability of high-volume-fly-ash- and slag-incorporated engineered cementitious composites," *ACI Materials Journal*, vol. 110, no. 3, pp. 259–267, 2013.

[24] M. Şahmaran, E. Özbay, H. E. Yücel, M. Lachemi, and V. C. Li, "Frost resistance and microstructure of engineered cementitious composites: influence of fly ash and micro poly-vinyl-alcohol fiber," *Cement and Concrete Composites*, vol. 34, no. 2, pp. 156–165, 2012.

[25] M. Öner, K. Erdoğdu, and A. Günlü, "Effect of components fineness on strength of blast furnace slag cement," *Cement and Concrete Research*, vol. 33, no. 4, pp. 463–469, 2003.

[26] M. Rostami and K. Behfarnia, "The effect of silica fume on durability of alkali activated slag concrete," *Construction and Building Materials*, vol. 134, pp. 262–268, 2017.

[27] P. Zhang and Q. F. Li, "Effect of silica fume on durability of concrete composites containing fly ash," *Science and Engineering of Composite Materials*, vol. 20, no. 1, pp. 57–65, 2013.

[28] P. Zhang and Q. F. Li, "Durability of high performance concrete composites containing silica fume," *Proceedings of the Institution of Mechanical Engineers Part L: Journal of Materials Design and Applications*, vol. 227, no. 4, pp. 343–349, 2013.

[29] P. Zhang and Q. F. Li, "Effect of polypropylene fiber on durability of concrete composite containing fly ash and silica fume," *Composites Part B: Engineering*, vol. 45, no. 1, pp. 1587–1594, 2013.

[30] M. T. Bassuoni and M. L. Nehdi, "Durability of self-consolidating concrete to sulfate attack under combined cyclic environments and flexural loading," *Cement and Concrete Research*, vol. 39, no. 3, pp. 206–226, 2009.

[31] T. P. Dolen, K. F. von Fay, and B. Hamilton, *Effects of Concrete Deterioration on Safety of Dams*, Dam Safety Office, Pretoria, South Africa, 2003.

[32] E. Özbay, O. Karahan, M. Lachemi, K. M. A. Hossain, and C. D. Atis, "Dual effectiveness of freezing–thawing and sulfate attack on high-volume slag-incorporated ECC," *Composites Part B: Engineering*, vol. 45, no. 1, pp. 1384–1390, 2013.

[33] Y. Cui, *Research on Uniaxial Compression Performance of Concrete under Freeze-Thaw Cycles and Carbonation*, Yangzhou University, Yangzhou, China, 2015.

[34] B. Larsone, *Toughness*, NDT Education Resource Center. The Collaboration for NDT Education, Iowa State University, Ames, IA, USA, 2011.

[35] E. H. Yang, Y. Z. Yang, and V. C. Li, "Use of high volumes of fly ash to improve ECC mechanical properties and material greenness," *ACI Materials Journal*, vol. 104, no. 6, pp. 620–628, 2007.